JOURNAL OF CHEMICAL & ENGINEERING DATA

ARTICLE

pubs.acs.org/jced

Biosorption of Methylene Blue from Aqueous Solution Using Lawny Grass Modified with Citric Acid

Lihua Chen,[†,‡] Anas Ramadan,[†] Lili Lü,[†] Wenjing Shao,[†] Fang Luo,[*,†] and Ji Chen[§]

[†]Key Laboratory of Polyoxometalates Science of Ministry of Education, College of Chemistry, Northeast Normal University, Changchun, 130024, China

[‡]Department of Chemistry, Heihe University, Heihe, 164300, China

[§]ChangChun Institute of Applied Chemistry, Chinese Academy of Sciences, Changchun, 130022, China

ABSTRACT: Using the low cost of lawny grass to remove methylene blue (MB) from aqueous solution was evaluated in the batch process and the fixed-bed column. The MB adsorption capacity onto CG (grass modified with citric acid) was 301.1 $mg \cdot g^{-1}$ biomass, which was almost three times than that of RG (raw grass). The equilibrium could be explained as pseudofirst-order kinetic processes, and equilibrium time was shortened to 20 min (CG) from 40 min (RG). The adsorption equilibrium followed the Langmuir isotherm model. The desorption rate with 0.1 $mol \cdot L^{-1}$ HCl was almost 90 %. Regenerated CG was reusable with a little decrease (only about 3.38 %) in its adsorption capacity during six repeated cycles. In the fixed-bed column, the breakthrough point of CG begins at 183 BV, which was much higher than that of RG (56 BV). The elution process was achieved in a very small HCl volume.

1. INTRODUCTION

Dyes are colorful organic compounds, which are released into environment through industrial effluent water of many industries;[1] dyeing effluents constitute one of the most problematic wastewaters not only for their high chemical and biological oxygen demands, but also for color, which, being visible to human eye, is the first contaminant to be recognized.[2] There are many structural varieties of dyes, such as acidic, basic, cationic, anionic, and so forth. Basic dyes are widely used in acrylic, nylon, silk, and wool dyeing. Most of these dyes are toxic, mutagenic, and carcinogenic.[3] Methylene blue (MB) is among the cationic adsorbates, its use being proposed as far back as 1924 by Paneth and Radu.[4] Though MB is not strongly hazardous, it can cause some harmful effects. Acute exposure to MB will cause increased heart rate, vomiting, shock, Heinz body formation, cyanosis, jaundice, quadriplegia, and tissue necrosis in humans.[5] Therefore, it is extremely important to remove it from industrial effluents before discharging it into the environment.

In recent years, more and more investigations have focused on the biosorption of MB by low-cost adsorbents derived from agricultural byproduct such as chaff,[6] rice straw,[7] mango seed,[8] wheat shells,[9] palm kernel fiber,[10] and so on. Lawny grass is regarded as a significant waste disposal problem. Although they can be used as animal feed, energy fuel, or compost, and so forth, it is better to utilize this waste material by turning it into a resource. Cellulose grass is a remarkable pure organic polymer, consisting solely of units of anhydroglucose held together in a giant straight chain molecule,[11] which is a crystalline homopolymer of glucose with $\beta 1-4$ glycosidic linkage and intramolecular and intermolecular hydrogen bonds.[12] Cellulose grass includes alcohols, aldehydes, ketones, carboxylic, phenolic, and ether groups. These groups will boast its ability, to some extent, to bind cationic dyes by donation of an electron pair from these groups to form complexes with the cationic dye in solution.[13]

In this sense, the main aim of our present work is to study the possibility of obtaining materials, having the adsorbent properties from lawny grass by adopting a treatment method. The adsorption capacity depends not only on the porous structure of the adsorbent, but also on its chemical composition and surface functional groups. Therefore, to improve the performance of the grass, it was modified with citric acid which introduces lots of functional carboxyl groups as proposed by Vaughan et al.[14] and Leyva-Ramos et al.[15] In this work, the adsorption properties of MB onto raw grass (RG) and grass modified with citric acid (CG) were compared by means of batch adsorption tests and dynamic column tests.

2. MATERIALS AND METHODS

2.1. Instrumentation and Reagents. The morphology of the samples was observed using a field-emission scanning electron microscope (FE-SEM, Hitachi S-4800). The elemental analysis of the raw lawny grass was carried out using GmbH Elementar. The sample was heated in an oven from 25 °C up to 1000 °C at a heating rate of 10 $°C \cdot min^{-1}$. The gases generated from heating were analyzed by an electrical conductivity detector. Fourier transform infrared spectroscopy (FT-IR) of both the raw and the modified lawny grass adsorbents was measured with a FT-IR spectrometer (Nicolet MagNAIR 560-spectrophotometer) under ambient conditions. The spectra were recorded from (4000 to 500) cm^{-1} using a KBr window. The thermogravimetric (TGA) and differential thermogravimetric (DTA) analyses of RG were performed on a Perkin-Elmer TGA-7 instrument in O_2 atmosphere with a heating rate of 10 $°C \cdot min^{-1}$.

Received: April 14, 2011
Accepted: June 28, 2011
Published: July 11, 2011

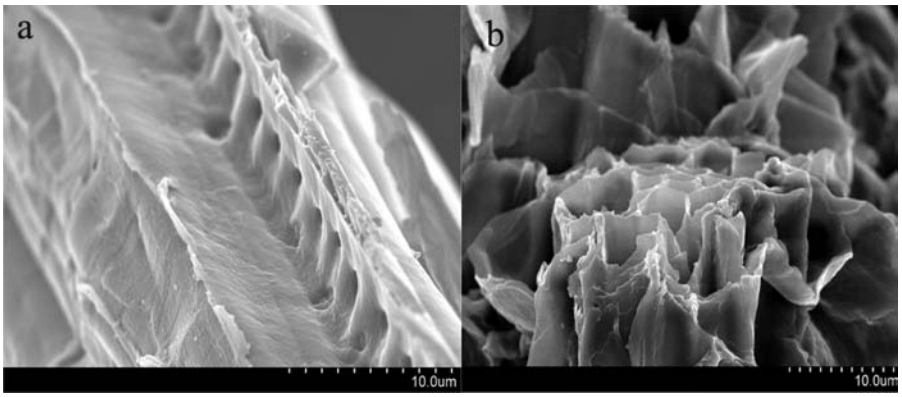

Figure 1. SEM images of RG (a) and CG (b).

A stock solution of 1000 mg·L^{-1} was prepared by dissolving accurately weighed samples of dye in a liter of distilled water. The working solutions were prepared by diluting the stock solution with distilled water to give the appropriate concentration of the solutions. The initial pH of each solution was adjusted with 0.1 mol·L^{-1} HCl or NaOH and measured with a pH s-3C model acidity meter (Shanghai Precision & Scientific Instrument Co. Ltd. China). All chemical agents used in this study were analytical grade, and all solutions were prepared with distilled water.

2.2. Preparation of Biosorbents. *2.2.1. Raw Material.* Grass was collected from the campus lawn, which was washed with water to take out silt, sand, and insoluble impurities, which was then dried for 12 h in a convection oven at a temperature of 60 °C. The dried grass was milled with a mill, and smaller particles were obtained by a sieve of 0.25 mm diameter. To a sample of 30 g of dried grass, 700 mL of 20 % isopropyl alcohol was added, and this grass was allowed to stand for 24 h at room temperature to remove some organic components like chlorophyll pigments and other low molecular-weight compounds such as limonene and so on; then the sample was filtered and washed with distilled water until the filtrate had no color. The residue was dried in an oven at 60 °C for 12 h and used in our experiments as a raw material, hereafter abbreviated as RG.

2.2.2. Modification with Citric Acid. A sample of 4 g of RG and 100 mL of 1.0 mol·L^{-1} citric acid solution were mixed in a beaker and stirred at 60 °C for 2 h and then filtered and dried in a convection oven at 60 °C for 12 h; in succession the temperature was increased up to 120 °C for 3 h. After that, the product was washed again and again with distilled water until pH was neutral. Finally, it was dried in an oven at 60 °C for 12 h. This was used as the modified grass hereafter abbreviated as CG.

2.3. Batch Adsorption Experiments. Batch adsorption tests were carried out at room temperature and used to investigate the effects of various parameters on MB adsorption by adsorbents. The experiments were conducted in 15 mL of MB solution (initial concentration 60 mg·L^{-1}) at different pH values (2.0 to 11.0), contact times [(3, 5, 8, 11, 15, 20, 30, 40, 60, 120, and 240) min], and adsorbent doses [(0.005, 0.015, 0.025, 0.035, 0.045, and 0.055) g]. Adsorption equilibrium experiments were carried out by adding a fixed amount of adsorbent (0.015 g) into a number of 50 mL stoppered glass (Erlenmeyer flasks) containing a definite volume (15 mL in each case) of different initial concentrations [(40 to 320) mg·L^{-1}] of dye solution without changing the pH. The dye solution was centrifuged at 5000 rpm for 5 min, and then residual concentration of MB was estimated using the spectrophotometric technique at the wavelength of 665 nm. The adsorption capacity (q) and removal efficiency (E %) are calculated according to eqs 1 and 2:

$$q = \frac{(C_0 - C_e)V}{W} \quad (1)$$

$$E\% = \frac{C_0 - C_e}{C_0} \cdot 100 \quad (2)$$

where C_0 and C_e are initial concentration and equilibrium concentrations of MB in the aqueous phase, respectively (mg·L^{-1}), q is the adsorption capacity (mg·g^{-1}), W is the mass of adsorbent (g), and V represents the volume of the aqueous phase (L).

2.4. Desorption and Reuse of Regenerated Biosorbents. Batch desorption tests using different concentrations of HCl were conducted to select the optimal concentration of HCl as the eluent in the column tests. After the 0.015 g sample of adsorbent loaded with MB was mixed with 15 mL of (0.005, 0.01, 0.05, 0.1 or 0.2) mol·L^{-1} HCl solution in an Erlenmeyer flask, the mixture was shaken in a rotary shaker for 4 h to reach equilibrium. After centrifugation at 5000 rpm for 5 min, the sample was dried and used for the next adsorption text on the same condition.

2.5. Column Experiments. The same amount of RG or CG was filled into two glass columns with a 1.1 cm diameter and 21.5 cm length. A small amount of glass wool was placed at the bottom and top of the column to prevent any loss of the adsorbent particles during the loading of MB. The column was fixed at the height of 4.0 cm and then conditioned by passing water of pH = 6.0 before MB loading. A solution of 100 mg·L^{-1} MB with an initial pH = 6.0 was pumped down-flow through the fixed-bed column at a constant volume velocity of 1 mL·min^{-1}. The effluent was collected regularly, and the concentration of MB was analyzed. After one point the concentration of MB was invariable, so we determined this point as the saturation point. After adsorption reached saturation, the columns were prewashed with distilled water so as to expel any unbound MB. HCl solution was used as eluent and percolated into the adsorbed columns at the same constant flow rate. After elution, columns were rinsed with distilled water until the pH reached the pH value of initial MB solution in the process of adsorption.

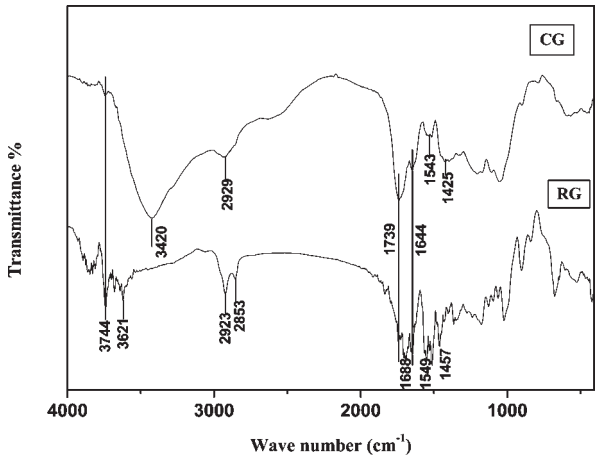

Figure 2. FT-IR spectra of RG and CG.

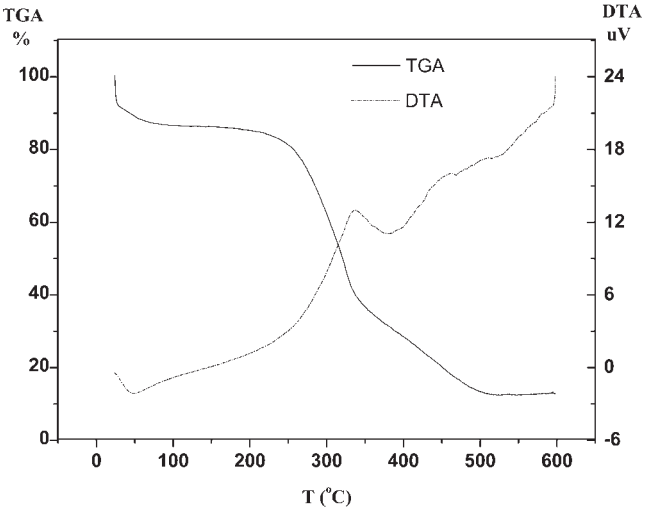

Figure 3. TGA and DTA curves of the RG.

3. RESULTS AND DISCUSSION

3.1. Characterization of Biosorbents. Figure 1 shows SEM images of RG (a) and CG (b). As compared with RG, the surface of CG is more irregular and porous, indicating that the surface area and pore volume increased. These large pores and increased surface area are important factors to enhance uptakes of MB. Elemental analysis results show that the raw lawny grass is composed of 43.69 % carbon, 5.63 % hydrogen, and 3.64 % nitrogen.

To better understand the change of surface functional groups after chemical modification, a comparison of the FT-IR spectrum of RG and CG is shown in Figure 2. The FT-IR spectra of RG shows that the doublet peaks at wavenumbers of 2954 cm^{-1} and 2853 cm^{-1} are due to the asymmetric and symmetric stretch of aliphatic chains (−CH), the three peaks at (1738, 1688, and 1644) cm^{-1} are the adsorption bands of carbonyl (C═O) stretching and hydroxyl (−OH) deformation vibration of carboxylic groups, the peak at 1549 cm^{-1} corresponds to the amide, and the peak at 1457 cm^{-1} is the symmetric C═O stretching. For the CG, it is observed that the peak at 1738 cm^{-1} stayed in position, but the peak at 1688 cm^{-1} disappeared. The amide vibration shifts from (1549 to 1543) cm^{-1}, hydroxyl (−OH) of

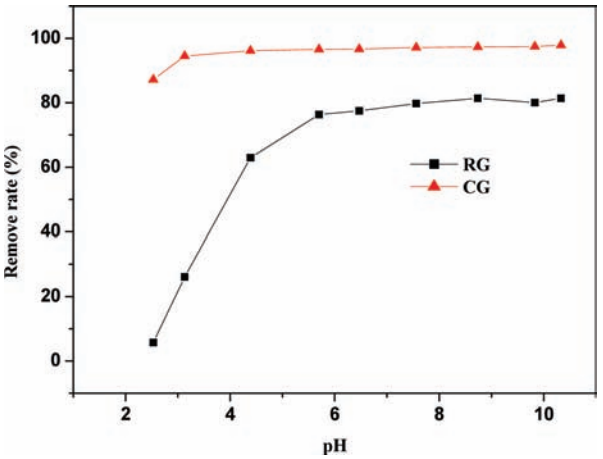

Figure 4. Effect of pH on MB uptake onto RG and CG. s/l ratio = 1 $g \cdot L^{-1}$; initial MB concentration = 60 $mg \cdot L^{-1}$; contact time = 4 h.

carboxylic groups shifts a little from (1644 to 1643) cm^{-1}, alkyl (−CH) shifts from (2923 to 2929) cm^{-1} and become a broad peak, and hydroxyl (−OH) appear at a wavenumber of 3425 cm^{-1}. The appearance and disappearance of different peaks indicates that some functional groups (−COOH and −OH) have been successfully introduced into the surface of the cellulose grass after chemical modification. These functional groups are very effective in capturing MB from aqueous solution.

Figure 3 shows the TGA and DTA curves of RG. The first decomposition process, which took place at around 100 °C, is attributed to the desorption of water molecules from the surface of the composites, and DTA data showed an abroad endothermic peak at about 100 °C. The weight loss observed in first decomposition step was about 15 %. The second weight loss observed at the plateau between (240 and 500) °C can be interpreted in term of a decomposition of the oxygenated surface groups. Meanwhile, a exothermic peak occurred at 340 °C. This mass loss is about 73 % for RG.

3.2. Effect of pH on Adsorption. The pH of aqueous solution exerts a profound influence on the sorption uptake of dyes presumably due to its impact on both the surface binding-sites of the biosorbent and the ionization/aggregation process of the dye molecules.[16] In the present biosorption system, Figure 4 shows the solution's pH effect in percentile on its efficiency of MB removal at various initial solution pH values between 2 and 10 for an initial dye concentration of 60 $mg \cdot L^{-1}$ and adsorbent dose of 1 $g \cdot L^{-1}$. At pH = 3, the removal efficiency of CG was 87.2 %, which is much higher than that of RG (5.74 %). At lower pH, the concentration of H^+ is higher, which competes with MB ions for surface active sites, so the removal efficiency of MB onto RG is very little. However, the CG still shows a higher removal efficiency, indicating that the citric acid has played a great role in the adsorption process. A sharply increase of MB uptake occurs after pH = 3.0, and the maximum uptake of MB onto CG could be up to 100 %, which was higher than that of RG (almost 80 %) in pH range of 6 to 10, and there was no significant difference in the dye concentration remaining when the pH was increased from 4.0 to 10.0.

The point of zero charge (PZC) also can be used to explain the effect of pH on MB adsorption. The determined method of PZC has been used satisfactorily by Leyva-Ramos et al.[15] and Moreno-Castilla et al.[17] At pH = PZC, the surface charge of adsorbents is

Table 1. Concentration of Active Sites and Point of Zero Charge (PZC)

	acidic sites	basic sites	
sorbent type	mol·kg^{-1}	mol·kg^{-1}	PZC
RG	0.75	2.25	6.38
CG	6.20	1.70	3.60

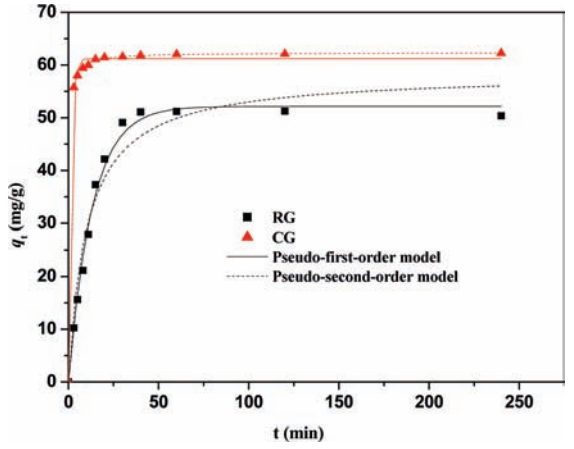

Figure 5. Effect of contact time on MB uptake and adsorption kinetics onto RG and CG. Initial pH = 5.7; s/l ratio = 1 g·L^{-1}; initial MB concentration = 60 mg·L^{-1}.

neutral; it is negligible of electrostatic attraction existing between the adsorbent surface and MB cations in solution. When pH > or < PZC, the balance is broken. At pH < PZC, the surface charge of adsorbents is positive, which inhibits the approach of positively charged MB cations. At pH > PZC, the surface charge of adsorbents is negative, and functional groups such as carboxyl, hydroxyl, and amino are free so as to promote interaction with MB cations. Maximum sorption is likely to occur at pH values greater than PZC when adsorbents have a net negative charge.[18] The rule of PZC agrees with adsorption behaviors of adsorbents. As can be seen from Table 1, the PZC of CG is 3.60, which is lower than that of RG (6.38), so CG has the stronger adsorption capacity than RG at a lower pH range. In addition, it can also be seen that the concentrations of acid site is higher than that of basic sites for CG, but which is not for RG; hence the surfaces of CG are acidic, and the number of acidic sites indicated the number of functional groups in the adsorbent.[19] These results are in accordance with our experimental results, as shown in Figure 3.

3.3. Effect of Contact Time on MB Uptake and Adsorption Kinetics. The contact time was also evaluated as an important factor of the adsorption efficiency. Figure 5 presents the effects of contact time on MB uptake onto RG and CG. It is clearly seen that the adsorption rate of MB increases rapidly with the increase of contact time before 20 min, then becomes slower with the increase of contact time until equilibria are achieved. When the contact time is 3 min, the sorption rate of MB onto CG is 86.13 %, which is approximately six times higher than that of RG (15.82 %). The equilibrium time was shortened to 20 min (CG) from 40 min (RG), which may be attributed to the additional ion exchange capacity of functional groups (−COOH) of citric acid.

To analyze the adsorption kinetics of MB, the pseudofirst-order[20] and pseudosecond-order[21] kinetics models were applied

Table 2. Pseudofirst-Order and Second-Order Kinetic Models for the Adsorption of MB

	pseudofirst-order model			pseudosecond-order model		
		q_e	K_1		q_e	K_2
biosorbent	R^2	mg·g^{-1}	L·min^{-1}	R^2	mg·g^{-1}	g·(mg·min)$^{-1}$
RG	0.9928	53.15	0.07625	0.9576	58.43	0.00167
CG	0.9999	61.21	0.7616	0.9869	62.35	0.04386

to fit the data, and nonlinear fitting was performed to determine the model parameters. The pseudofirst-order kinetic model was generally expressed as eq 3:

$$\ln \frac{q_e - q_t}{q_e} = -K_1 t \tag{3}$$

where q_t and q^e are the capacity of MB adsorbed (mg·g^{-1}) at time t (min) and equilibrium, and K_1 is the pseudofirst-order rate constant (min^{-1}).

The pseudosecond-order kinetic model was expressed as the following formulation:

$$\frac{t}{q_t} = \frac{1}{K_2 q_e^2} + \frac{t}{q_e} \tag{4}$$

where K_2 is the pseudosecond-order rate constant (g·(mg·min)$^{-1}$).

The kinetic model parameters are obtained from fitting results and are presented in Table 2. The pseudofirst-order kinetic model provides much better R^2 values (0.9928 and 0.9999) than that of the pseudosecond-order kinetic model (0.9576 and 0.9869), indicating that the pseudofirst-order equation was the best fit for the experimental kinetic data. The nonlinear kinetics equations were preferred over linear equations, since the latter does not take into account the errors associated with each experimental point, which cannot always be linearized.[22] The pseudofirst-order model describes adsorption reactions at the particle−solution interface and frequently shows biphasic kinetics with a fast rate at the beginning followed by a slower rate. Accordingly, the experimental data can be described by two-phase pseudofirst-order reaction behavior, which may be interpreted as reactions on two types of sites, namely, external sites that are quickly accessible and internal sites that are less accessible and show slower rates of sorption.[23,24] At the first fast adsorption phase, the adsorption rate of MB increases rapidly with the increase of contact time before 20 min due to the rapidly cell-surface binding with MB. At the second adsorption phase, the adsorption process is suspected that the uptake of MB by the lawny grass was probably not only due to cell-surface binding, but also via intracellular accumulation.[25] This possibility is explored by plotting of uptake (q_t) versus the square root of time ($t^{1/2}$), according to the Weber−Morris model,[26] $q_t = K^{id}\, t^{1/2}$, where K_{id} is the intraparticle diffusion coefficient. The plot of q_t versus $t^{1/2}$ should be linear if intraparticle diffusion is involved in the adsorption process, and if these lines pass through the origin, then intraparticle diffusion is the rate-controlling step. When the plots do not pass through the origin, this is indicative of some degree of boundary layer control, and it further shows not only that the intraparticle diffusion is the rate-limiting step, but also that other kinetic models may control the rate of adsorption, all of which may be operating simultaneously.[27] The plots of q_t versus $t^{1/2}$ are presented in

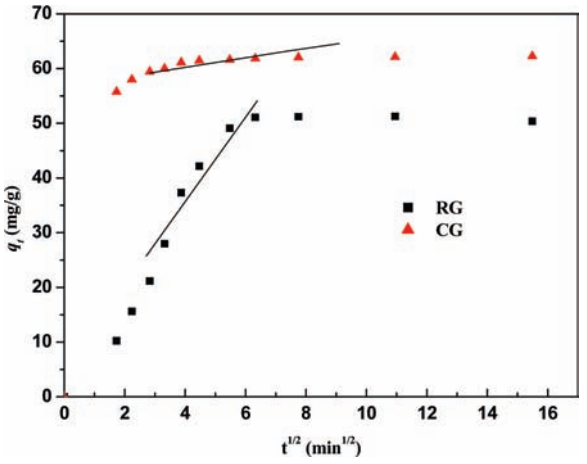

Figure 6. Intraparticle diffusion plot of MB adsorption onto RG and CG. Initial pH = 5.7; s/l ratio = 1 g·L^{-1}; initial MB concentration = 60 mg·L^{-1}.

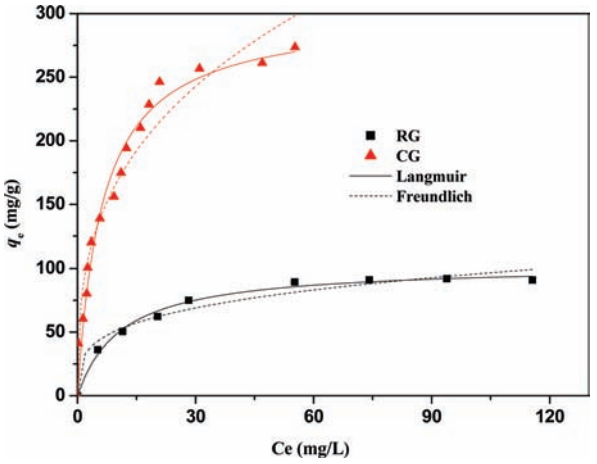

Figure 7. Langmuir and Freundlich adsorption isotherms of MB onto RG and CG. Initial pH = 5.7; s/l ratio = 1 g·L^{-1}; contact time = 4 h.

Figure 6. It can be seen that these plots do not pass through the origin, indicating that the intraparticle diffusion is not the only rate-controlling step.

3.4. Adsorption Isotherms. In this part, the relationships between the initial concentration of MB and the adsorbed amount of MB onto CG and RG are studied and presented in Figure 7. It can be seen from these curves that the adsorption uptakes of MB increase with the increase of equilibrium concentration of MB and then reach a plateau. It is attributed to the surface active sites of adsorbents which have become saturated.

Two isotherms were tested for their ability to describe the experimental results, namely, the Langmuir[28] and Freundlich[29] adsorption isotherms. The thermodynamic assumptions of the best fitting isotherm provide insight into both the surface properties and the mechanism of adsorption. The derivation of the Langmuir isotherm is based on the assumption of ideal monolayer adsorption on a homogeneous surface. It is expressed by the following equation:

$$q_e = \frac{q_m b C_e}{1 + bC_e} \quad (5)$$

Table 3. Equilibrium Isotherm Constants for the Sorption of MB onto RG and CG

	Langmuir			Freundlich		
		b	q_m		K_f	
biosorbent	R^2	L·mg^{-1}	mg·g^{-1}	R^2	L·g^{-1}	n
RG	0.9814	0.09005	103.0	0.9235	27.66	3.718
CG	0.9691	0.1569	301.1	0.9469	77.08	2.964

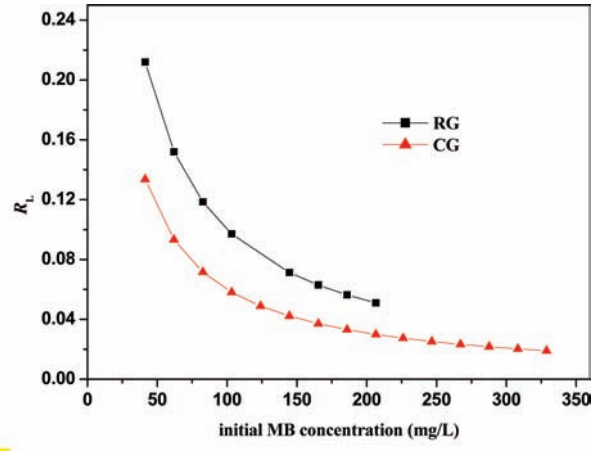

Figure 8. Value of separation factor (R_L) for the sorption of MB by RG and CG.

where q_e and q_m (mg·g^{-1}) are the equilibrium and maximum adsorption amounts of MB per unit weight of adsorbent, respectively; b represents the equilibrium constant of adsorption reaction (L·mg^{-1}), while c_e (mg·L^{-1}) is the concentration of adsorbate at equilibrium.

The Freundlich isotherm is used for nonideal adsorption on heterogeneous surfaces. The heterogeneity is caused by the presence of different functional groups on the surface and also by various mechanisms of adsorbent−adsorbate interactions. The Freundlich isotherm is represented by the following empirical equation:

$$q_e = K_f C_e^{1/n} \quad (6)$$

where K_f and n are the Freundlich constants, K_f is roughly an indicator of the adsorption capacity (L·g^{-1}), and $1/n$ is an empirical parameter relating the adsorption intensity.

The fitting results are also shown in Figure 7, and the parameter values are listed in Table 3. The regression correlation coefficients (R^2) values of Langmuir isotherms are 0.9814 and 0.9691 for MB adsorption on RG and CG, respectively, which are higher than that of the Freundlich isotherm (0.9235 and 0.9469), indicating that the Langmuir model was more suitable for describing the adsorption equilibrium data of MB by grass biomass in the studied concentration range. In other words, this adsorption process took place at the functional groups/binding sites on the surface of adsorbents which is regarded as monolayer adsorption. Also Langmuir parameters can be used to predict affinity between the adsorbate and the

dx.doi.org/10.1021/je200366n |J. Chem. Eng. Data 2011, 56, 3392–3399

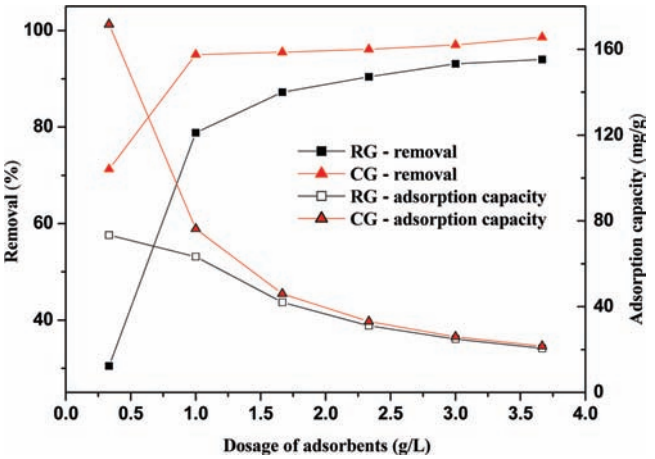

Figure 9. Effect of adsorbents dosage on the adsorption of MB onto RG and CG. Initial pH = 5.7; initial MB concentration = 80 mg·L^{-1}; contact time = 4 h.

Table 4. Comparison of MB Uptake onto CG and Other Adsorbents

adsorbent	t °C	equilibrium time h	pH	q_m mg·g^{-1}	refs
CG	25	1/3	5.7	301.1	this study
pomelo peel	30	5.15	7	344.8	38
Phellinus igniarius	20	48	7.5	204.4	37
Jalshakti polymer	25	2	5.5	172.4	36
mango seed kernel	25	48	8	153.8	39
sewage sludge	25	3	–	114.9	40
Nuchar C-190 AC[a]	25	2	6	104.2	36
coconut bunch waste	30	5.15	7	70.92	41
rice husk	32	48	8	40.59	42
coconut coir dust AC[a]	25	2	8	14.36	43
orange peel	30	24	>7	13.9	44

[a] AC: activated carbon.

adsorbent using the dimensionless separation factor (R_L), given by eq 7:

$$R_L = \frac{1}{1 + bC_0} \quad (7)$$

where R_L is the dimensionless separation factor, C_0 is the initial concentration of the adsorbate (mg·L^{-1}), and b is the Langmuir constant (L·mg^{-1}). The R_L value can be used to predict whether a sorption system is "favorable" or "unfavorable".[30,31] If the average values of the R_L are between 0 and 1 at different initial concentrations, it indicates favorable adsorption.[32] The R_L values for sorption of MB on RG and CG are shown in Figure 8. In our experiments, all values of R_L are in the range of 0 and 1 at all initial dye concentrations, indicating that the adsorption of MB onto grass was a favorable process. According to the Langmuir isotherm model, the maximum dye adsorption capacity of CG was found to be 301.1 mg·g^{-1} biomass, which is almost three times than that of RG (103.0 mg·g^{-1}).

3.5. Effect of Adsorbent Dosage on MB Adsorption. The removal rate (%) and adsorption capacity (mg·g^{-1}) of MB at different doses of RG and CG are shown in Figure 9. It is observed that an increase in the mass of adsorbents results in the increase of MB removal rate; this can be attributed to increased adsorbent surface area and availability of more adsorption sites. However, a decrease in adsorption capacity can be explained with the reduction in the effective surface area.[33−35] As seen from Figure 9, the removal rate of MB onto CG increased from 71.3 % to 98.6 % when the adsorbent load increased from (0.33 to 3.67) g·L^{-1}, and the removal rate easily reaches maximum just at 1 g·L^{-1}, whereas it reaches a maximum at 3 g·L^{-1} for RG, suggesting that the grass after modification greatly reduced the use of adsorbent. In terms of removal percent and cost effect, the optimum adsorbent dosage of CG is 1 g·L^{-1} for practical applications.

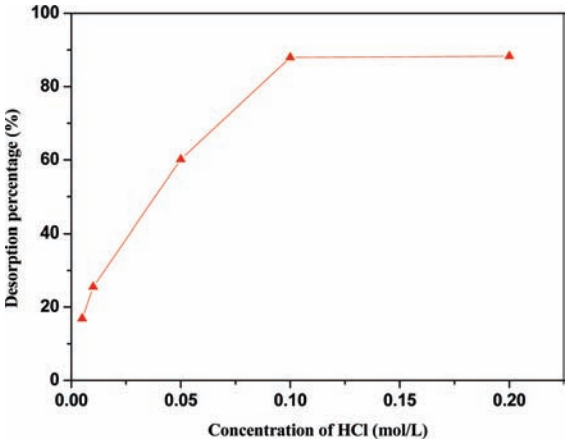

Figure 10. Effect of concentration of HCl on desorption percentage by CG. s/l ratio = 1 g·L^{-1}; contact time = 4 h.

Table 5. Adsorption−Desorption Recycles of CG

recycle times	1	2	3	4	5	6
adsorption rate[a] (%)	96.28	95.59	94.83	94.06	93.48	92.90
desorption rate[b] (%)	89.60	89.58	88.29	90.70	91.61	91.16

[a] Initial pH = 5.7; initial MB concentration = 94.99 mg·L^{-1}; s/l ratio = 1 g·L^{-1}. [b] 0.1 mol·L^{-1} HCl was used as a desorption agent.

3.6. Comparing the Sorption Capacity of CG with Other Sorbents. To show the very high sorption capacity of MB onto CG biosorbent, an exhaustive comparison with other biosorbents was made. The results, illustrated in Table 4, showed that, with a sorption capacity of about 301.1 mg·g^{-1}, the CG is a very performing and promising biomaterial to remove MB even compared with other sorbents, such as activated carbons. For instance, CG biomass is able to adsorb nearly three times more than a commercial activated carbon (104 mg·g^{-1}).[36] Thus, low cost, available, and renewable chemical modified grass seems to be very competitive to other MB-sorbent materials.

3.7. Desorption and Reuse of CG. An adsorbent with a fine regeneration capacity can reduce pretreatment costs and improve the reusability of a biosorbent which is of critical significance in practical applications for dye removal from wastewaters. Therefore, the adsorption capacity of dye onto CG was determined by repeated adsorption−desorption cycles. In this study, desorption experiments were conducted under different concentrations of HCl. From Figure 10, the percentages of desorption increased with increasing HCl concentration from (0.005 to 0.1) mol·L^{-1} and then changed little. Therefore, 0.1 mol·L^{-1} HCl

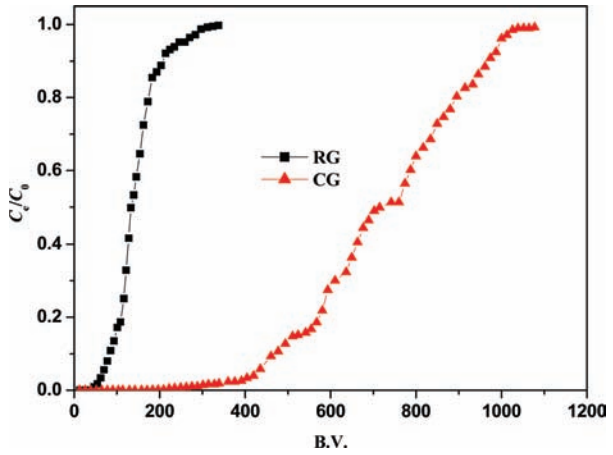

Figure 11. Breakthrough curves of adsorption MB in the columns of RG and CG. Initial MB concentration = 100 mg·L^{-1}; initial pH = 6.0; constant volume velocity = 1 mL·min^{-1}.

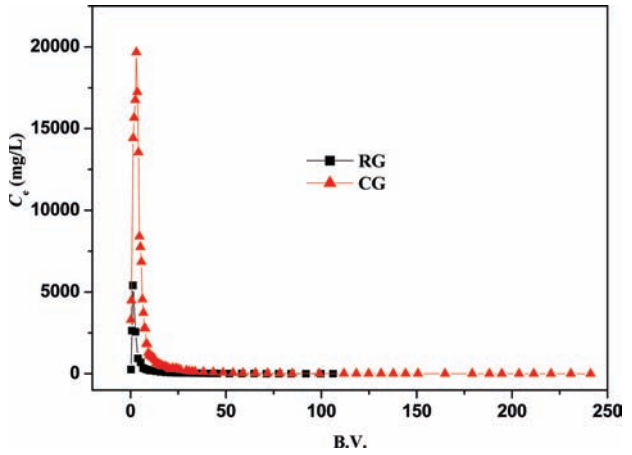

Figure 12. Elution curves of MB using 0.1 mol·L^{-1} HCl in the columns of RG and CG.

solution was regarded as the optimum eluent to regenerate the adsorption column. The CG still retain good MB adsorption capacity even after six cycles. After the sixth cycle, the adsorption rate of MB onto CG was still 92.90 % (Table 5), and the total decreases in sorption efficiency of CG after six adsorption−desorption cycles was only about 3.38 %, indicating that CG has good potential to adsorb MB from aqueous solution even when used repeatedly.

3.8. Column Studies. Adsorption in a fixed-bed column was widely used and considered as fundamental for further studies involving the scaling-up of the process under actual conditions. The experimental breakthrough curves are used to calculate the column capacity at complete exhaustion, which is usually greater than in the batch experiments.[45] Breakthrough curves of MB adsorption on RG and CG are presented in Figure 11. It can be seen that the breakthrough point begins at 56 BV for RG; however, it begins at 183 BV for CG. Here, BV is defined as a volume ratio of MB solution which passes through the column (cm^3) to the packed adsorbents (cm^3). The column of RG is completely saturated at 337 BV, and that of CG is completely saturated at 1064 BV. This result indicates that the adsorption capacity of the modified grass for MB showed a significant increase compared with the unmodified grass due to the presence of a large number of carboxyl groups.

With a high elution efficiency of almost 90 %, 0.1 mol·L^{-1} of HCl was noted to perform well in the elution of MB from RG and CG. The elution breakthrough curves of the column MB-loaded RG and CG are presented in Figure 12. It may be noted from the breakthrough curves that MB concentration in the effluent increased sharply during the initial stage and reached the maximum values of 5402 mg·L^{-1} at 1.3 BV for RG and 19671 mg·L^{-1} at 3.1 BV for CG, respectively; then MB concentration decreased rapidly, and the elution process was completed within 108 BV and 241 BV for RG and CG, respectively. This resulted in a very highly concentrated MB solution elute in very small elutent HCl volume and allowed the recovery process to be easier.

4. CONCLUSIONS

The present study shows that the grass modified with citric acid can be used as an effective and competitive adsorbent for the removal of MB dye from aqueous solutions. The capacity of raw grass was greatly enhanced by pretreatment with citric acid, and the maximum dye biosorption capacity of RG and CG was found to be (103.0 and 301.1) mg·g^{-1} biomass, respectively. The equilibrium time was shortened to 40 min (CG) from 60 min (RG). The CG had a fine regeneration and reuse capacity, as the total decreases in sorption efficiency after six adsorption−desorption cycles was only about 3.38 %, and the adsorption rate of MB onto CG was still 92.90 % at the sixth cycle. In the fixed-bed column process, the breakthrough point of CG begins at 183 BV, which was higher than that of RG (56 BV). The elution was complete by a very small HCl volume.

AUTHOR INFORMATION

Corresponding Author

*Tel.: +86 431 8889 3336. E-mail address: luof746@nenu.edu.cn.

Funding Sources

We thank the Training Fund of NENU's Scientific Innovation Project (NENU-STC08008), the Fundamental Research Funds for the Central Universities, and the Natural Science Foundation of Jilin Province (201115001).

REFERENCES

(1) Easton, J. R.; Waters, B. D.; Churchley, J. H.; Harrison, J. Colour in Dyehouse Effluent. In *Society of Dyers and Colourists*, Cooper, P., Ed.; The Alden Press: Oxford, 1995; p 9.

(2) Correia, V. M.; Stephenson, T.; Judd, S. J. Characterization of textile wastewaters: a review. *Environ. Technol.* **1994**, *15*, 917–919.

(3) Hameed, B. H.; El-Khaiary, M. I. Removal of basic dye from aqueous medium using a novel agricultural waste material: Pumpkin seed hull. *J. Hazard. Mater.* **2008**, *155*, 601–609.

(4) Barton, S. S. The adsorption of methylene blue by active carbon. *Carbon* **1987**, *25*, 351–359.

(5) Hameed, B. H.; Ahmad, A. A. Batch adsorption of methylene blue from aqueous solution by garlic peel, an agricultural waste biomass. *J. Hazard. Mater.* **2009**, *164*, 870–875.

(6) Han, R. P.; Wang, Y. F.; Han, P.; Shi, J.; Yang, J.; Lu, Y. S. Removal of methylene blue from aqueous solution by chaff in batch mode. *J. Hazard. Mater.* **2006**, *B137*, 550–557.

(7) Gong, R. M.; Zhong, K. D.; Hu, Y.; Chen, J.; Zhu, G. P. Thermochemical esterifying citric acid onto lignocellulose for enhancing methylene blue sorption capacity of rice straw. *J. Environ. Manage.* **2008**, *88*, 875–880.

(8) Vasanth Kumar, K.; Kumaran, A. Removal of methylene blue by mango seed kernel powder. *Biochem. Eng. J.* **2005**, *27*, 83–93.
(9) Bulut, Y.; Aydin, H. A kinetics and thermodynamics study of methylene blue adsorption on wheat shells. *Desalination* **2006**, *194*, 259–267.
(10) Ofomaja, A. E. Kinetics and mechanism of methylene blue sorption onto palm kernel fibre. *Process Biochem.* **2007**, *42*, 16–24.
(11) Demirbas, A. Mechanisms of liquefaction and pyrolysis reactions of biomass. *Energy Convers. Manage.* **2000**, *41*, 633–646.
(12) Demirbas, A. Recent advances in biomass conversion technologies. *Energy Educ. Sci. Technol.* **2000**, *6*, 19–41.
(13) Pagnanelli, F.; Mainelli, S.; Veglio, F.; Toro, L. Heavy metal removal by olive pomace: biosorbent characterisation and equilibrium modelling. *Chem. Eng. Sci.* **2003**, *58*, 4709–4717.
(14) Vaughan, T.; Seo, C. W.; Marshall, W. E. Removal of selected metal ions from aqueous solution using modified corncobs. *Bioresour. Technol.* **2001**, *78*, 133–139.
(15) Leyva-Ramos, R.; Bernal-Jacome, L. A.; Acosta-Rodriguez, I. Adsorption of cadmium(II) from aqueous solution on natural and oxidized corncob. *Sep. Purif. Technol.* **2005**, *45*, 41–49.
(16) Ncibi, M. C.; Ben Hamissa, A. M.; Fathallah, A.; Kortas, M. H.; Baklouti, T.; Mahjoub, B.; Seffen, M. Biosorptive uptake of methylene blue using Mediterranean green alga *Enteromorpha* spp. *J. Hazard. Mater.* **2009**, *170*, 1050–1055.
(17) Moreno-Castilla, C.; Lopez-Ramon, M. V.; Carrasco-Marin, F. Changes in surface chemistry of activated carbons by wet oxidation. *Carbon* **2000**, *38*, 1995–2001.
(18) Romero-Gonzalez, M. E.; Williams, C. J.; Gardiner, P. H. E. Study of the mechanisms of cadmium biosorption by dealginated seaweed waste. *Environ. Sci. Technol.* **2001**, *35*, 3025–3030.
(19) Boehm, H. P. Some aspects of the surface chemistry of carbon blacks and other carbons. *Carbon* **1994**, *32*, 759–769.
(20) Lagergren, S. Zur theorie der sogenannten adsorption geloster stoffe, Kungliga Svenska Vetenskapsakademiens. *Handlingar* **1898**, *24*, 1–39.
(21) Ho, Y. S. Adsorption of heavy metals from waste streams by peat. Ph.D. Thesis, University of Birmingham, Birmingham, U.K., 1995.
(22) Vaghetti, J. C. P.; Lima, E. C.; Royer, B.; Brasil, J. L.; da Cunha, B. M.; Simon, N. M.; Cardoso, N. F.; Norena, C. P. Z. Application of Brazilian-pine fruit coat as a biosorbent to removal of Cr(VI) from aqueous solution: Kinetics and equilibrium study. *Biochem. Eng. J.* **2008**, *42*, 67–76.
(23) Lugo-Lugo, V.; Hernandez-Lopez, S.; Barrera-Diaz, C.; Urena-Nunez, F.; Bilyeu, B. A comparative study of natural, formaldehyde-treated and copolymer-grafted orange peel for Pb(II) adsorption under batch and continuous mode. *J. Hazard. Mater.* **2009**, *161*, 1255–1264.
(24) Sparks, D. L. *Soil Physical Chemistry*, 2nd ed.; CRC Press: Boca Raton, FL, 1999.
(25) Bajpai, S. K.; Rohit, V. K. Cation exchanger sawdust (CESD) as an effective sorbent for removal of Cu (II) from aqueous solution. *EJEAFChe.* **2007**, *6*, 2053–2065.
(26) Weber, W. J.; Morris, J. C. Kinetics of adsorption on carbon solution. *J. Sanit. Eng. Div.* **1963**, *89*, 31–59.
(27) Hameed, B. H. Equilibrium and kinetic studies of methyl violet sorption by agricultural waste. *J. Hazard. Mater.* **2008**, *154*, 204–212.
(28) Langmuir, I. The constitution and fundamental properties of solids and liquids. *J. Am. Chem. Soc.* **1916**, *38*, 2221–2295.
(29) Freundlich, H. M. F. Uber die adsorption in lasugen. *Z. Phys. Chem.* **1906**, *57*, 385–470.
(30) Hall, K. R.; Eagleton, L. C.; Acrivos, A.; Vermeulen, T. Pore- and solid-diffusion kinetics in fixed bed adsorption under constant-pattern conditions. *Ind. Eng. Chem. Fundam.* **1996**, *5*, 212–223.
(31) Weber, T. W.; Chakravorti, P. K. Pore and solid diffusion models for fixed adsorbers. *AIChE J.* **1974**, *20*, 226–237.
(32) Vilar, V. J. P.; Botelho, C. M. B.; Boaventura, R. A. R. Methylene blue adsorption by algal biomass based materials: biosorbents characterization and process behaviour. *J. Hazard. Mater.* **2007**, *147*, 120–132.
(33) Wang, S.; Zhu, Z. H.; Coomes, A.; Haghseresht, F.; Lu, G. Q. The physical and surface chemical characteristics of activated carbons and the adsorption of methylene blue from wastewater. *J. Colloid Interface Sci.* **2005**, *284*, 440–446.
(34) Otero, M.; Rozada, F.; Calvo, L. F.; Garcıa, A. I.; Moŕan, A. Kinetic and equilibrium modelling of the methylene blue removal from solution by adsorbent materials produced from sewage sludges. *Biochem. Eng. J.* **2003**, *15*, 59–68.
(35) Waranusantigul, P.; Pokethitiyook, P.; Kruatrachue, M.; Upatham, E. S. Kinetics of basic dye (methylene blue) biosorption by giant duckweed (*Spirodela polyrrhiza*). *Environ. Pollut.* **2003**, *125*, 385–392.
(36) Dhodapkar, R.; Rao, N. N.; Pande, S. P.; Kaul, S. N. Removal of basic dyes from aqueous medium using a novel polymer: Jalshakti. *Bioresour. Technol.* **2006**, *97*, 877–885.
(37) Maurya, N. S.; Mittal, A. K.; Cornel, P.; Rother, E. Biosorption of dyes using dead macro fungi: Effect of dye structure, ionic strength and pH. *Bioresour. Technol.* **2006**, *97*, 512–521.
(38) Hameed, B. H.; Mahmoud, D. K.; Ahmad, A. L. Sorption of basic dye from aqueous solution by pomelo (*Citrus grandis*) peel in a batch system. *Colloids Surf., A* **2008**, *316*, 78–84.
(39) Kumar, K. V.; Kumaran, A. Removal of methylene blue by mango seed kernel powder. *Biochem. Eng. J.* **2005**, *27*, 83–93.
(40) Otero, M.; Rozada, F.; Calvo, L. F.; Garcia, A. I.; Moran, A. Kinetic and equilibrium modelling of the methylene blue removal from solution by adsorbent materials produced from sewage sludges. *Biochem. Eng. J.* **2003**, *15*, 59–68.
(41) Hameed, B. H.; Mahmoud, D. K.; Ahmad, A. L. Equilibrium modeling and kinetic studies on the adsorption of basic dye by a novel adsorbent: coconut (*Cocosnucifera*) bunch waste. *J. Hazard. Mater.* **2008**, *158*, 65–72.
(42) Vadivelan, V.; Kumar, K. V. Equilibrium, kinetics, mechanism, and process design for the sorption of methylene blue onto rice husk. *J. Colloid Interface Sci.* **2005**, *286*, 90–100.
(43) Macedo, J. S.; da Costa, N. B.; Almeida, L. E.; Vieira, E. F.; Cestari, A. R.; Gimenez, I. F.; Carrẽno, N. L.; Barreto, L. S. Kinetic and calorimetric study of the adsorption of dyes on mesoporous activated carbon prepared from coconut coir dust. *J. Colloid Interface Sci.* **2006**, *298*, 515–522.
(44) Annadurai, G.; Juang, R.; Lee, D. Use of cellulose-based wastes for adsorption of dyes from aqueous solutions. *J. Hazard. Mater.* **2002**, *B92*, 263–274.
(45) Lu, D. D.; Cao, Q. L.; Cao, X. J.; Luo, F. Removal of Pb(II) using the modified lawny grass: Mechanism, kinetics, equilibrium and thermodynamic studies. *J. Hazard. Mater.* **2009**, *166*, 239–247.